Available online at www.sciencedirect.com
Pergamon
Cement and Concrete Research 34 (2004) 1007–1015
CEMENT AND CONCRETE RESEARCH

Study of the Joule effect on rapid chloride permeability values and evaluation of related electrical properties of concretes

G.A. Julio-Betancourt, R.D. Hooton*
Department of Civil Engineering, University of Toronto, 35 St. George Street, Toronto, Ontario, Canada M5S 1A4
Received 29 May 2003; accepted 17 November 2003

Abstract

Concrete specimens were tested at different temperatures using the ASTM C1202 rapid chloride permeability test (RCPT). The influence of temperature on the RCPT results was analyzed and activation energies were calculated. An Arrhenius equation was presented to account for the Joule effect due to heating. Electrical properties of concrete derived from the test were evaluated and correlations were explained based on the effect of temperature on the kinetics of the pore fluid and on the microstructure of concrete. The results support the modification of ASTM C1202 by changing it to a 1-min conductivity test.

Keywords: Permeability; Electrical properties; Temperature; Concrete; Conductivity

1. Introduction

One of the main problems in concrete structures has been chloride-induced corrosion. Thus, an assessment of the rate of ingress of chlorides has become a very important property for assessing the long-term performance of concrete structures.

Since the 1970s different organizations and professionals have tried to develop and implement rapid, inexpensive and reliable tests to measure the ability of concrete to resist the penetration of chloride ions. Whiting developed one of these tests for the Federal Highway Administration (FHWA) in the late 1970s, and it is typically referred to as the rapid chloride permeability test (RCPT) [1,2], even though it is really a measure of electric conductivity. This test was adopted by AASHTO in 1983 as T277 and by ASTM in 1991 as ASTM C1202 [2].

The RCPT has been related to the diffusion of chloride ions [4,5]. The problem with some concretes is that high current levels result in heating during the test. The effect known as the Joule effect has been reported by Whiting [1,2] and other authors [6–19,23]. The temperature in the solution and concrete specimen increases during the test due to the flow of electric current generated by the relatively high applied voltage (60 V). The heating is more evident when the test is performed on young concretes or on those concretes with high water–cement ratios. Since electrical conductivity is sensitive to temperature, heating will result in higher measured coulomb values [25–33]. Trying to overcome this problem in the RCPT and similar chloride migration tests, some researchers have modified the size of the cell [8], used a lower voltage [4,11,13,19–21] or even proposed to run the test for only 30 min to reduce or eliminate the heating effect [4,22].

It is understood that the flow of electric current through a conductor generates heat (law of conservation of energy). This heat is proportional to the quantity of electricity or charge passed through the conductor and to the applied potential (Eq. (1)) [25–33]. The RCPT method requires obtaining the total charge passed in coulombs at the end of the test by integrating (or by using the trapezoidal rule) the electric current passed during the 6 h. Because the voltage and the time are kept constant in the RCPT, the electric current is the only variable.

$$J = EIt \tag{1}$$

where J is the heat (joules), E is the potential (volts), I is the current (amperes) and t is the time (seconds).

An incremental change in temperature will increase the mobility of all ions that carry the current, which in turn will

* Corresponding author. Tel.: +1-416-978-5912; fax: +1-416-978-6813.
E-mail address: hooton@civ.utoronto.ca (R.D. Hooton).

0008-8846/$ – see front matter © 2004 Elsevier Ltd. All rights reserved.
doi:10.1016/j.cemconres.2003.11.012

raise the total current flow producing more heat in a cyclic process.

On the other hand, the flow of electric current through concrete is mainly electrolytic in nature (through the pore fluid); therefore, based on early studies of electrolyte solutions, Ohm's law ($V=IR$) is expected to hold for concretes with some limitations: specifically, Ohm's law is not longer linear for high-potential gradients and high-frequency alternating currents due to (a) concentration changes in the electrolyte solution, (b) electrode polarization, (c) Wien effect and (d) the Debye–Falkenhagen effect [25–33]. These effects will cause some deviation from Ohm's law when it is applied to electrolyte solutions. However, concrete is a porous body with a resistance higher than that of the same volume of electrolyte solution alone, so some of these effects may be negligible. In the case of the RCPT, the last two effects are not applicable because of the use of a relative low direct current potential in the measurements (60 V DC). On the contrary, the first two effects still have an impact on the validity of Ohm's law, including the heat generated during the 6-h test. However, some authors have successfully used the RCPT to measure the conductivity of concrete (during the first 4 min) with a negligible error (less than 5%) [6]. In addition, potential drops have been reported to be less than 2.5 V for potentials up to 30 V [34]. Thus, Ohm's law is still likely valid for the RCPT as long as the temperature in the system is held constant.

Concrete can be considered an electrolytic conductor because it is through the pore fluid that most of the transport of current occurs [24]. Thus, the quantity of current passed through the concrete specimen will depend on the composition, concentration and the mobility of the ions present in the pore fluid in addition to the porosity and continuity of the pore system. Additionally, the influence of temperature on the resistivity of concrete is similar to those of semiconductors where the resistivity decreases with an increase in temperature [25].

In this project the Joule effect was studied and an equation developed to account for the heat effect on the total charge. Correlations of data extracted or derived from the RCPT related to the electrical properties of concrete (conductivity and resistivity) are presented and some insights into the possible changes in pore fluid conductivity and the concrete's microstructure are discussed.

2. Experimental work

2.1. Material and specimen preparation

Table 1 shows the general mix proportions for some concretes used in this study, including their age at test. The coarse aggregate was 10 mm crushed limestone and the fine aggregate was glacial sand with a fineness modulus of 2.75. Concrete specimens were either 100-mm-diameter cores extracted from small concrete slabs ($400 \times 275 \times 75$ mm) or from cylinders (100×200 mm). Cores and cylinders were sawn to a thickness of 51 ± 3 mm. Corrections to results were made to base them on the standard diameter of 95 mm as outlined in ASTM C1202.

2.2. Experimental procedure

Basically, all the experiments were done following the ASTM C1202-97 standard [3]. An RCPT instrument (Germann Instruments) was used to obtain the total charge or RCPT values of some of the concrete specimens. This instrument allows testing up to eight cells at the same time and includes thermistor probes to measure the temperature of the solution in each cell. Some concrete specimens were tested in a different instrument system (RLC Instruments), and the temperature during these experiments was monitored using thermometers immersed in both cells.

As part of this study, specimens from six different types of concrete were exposed to artificial heating regimes. In these cases, an assembled cell was immersed in water and then heated up to a specific temperature in the range of 50 to 90 °C using a programmable water bath with a digital controller to control the temperature of the bath fluid accurately. The water bath could be controlled over the range of -30 to 130 ± 0.01 °C, and additional thermometers (located in both sides of the cell) were used to record

Table 1
Proportions and ages of concrete mixtures for temperature regime experiments

Materials	Mix code								
	G	M	A	E	T'	T	W	C7	C13
CSA Type 10 (kg/m^3)	263	375	76.8	355	–	–	363	266.8	500
CSA Type 30 (kg/m^3)	–	–	–	–	300	400	–	–	–
Slag (kg/m^3)	–	–	38.4	–	–	–	–	–	–
Fly ash (C) (kg/m^3)	–	–	–	–	100	–	–	72.5	–
Silica fume (kg/m^3)	–	–	76.8	–	–	–	–	23.2	42
W/C$_m$	0.6	0.4	0.79	0.38	0.35	0.35	0.45	0.45	0.25
Coarse/Fine (kg/m^3)	1067/944	1100/787	1135/771	1100/830	1155/743	1155/756	1025/707	1025/668	1130/675
Coarse/Fine (%)	53/47	58/42	60/40	57/43	61/39	60/40	59/41	60/40	63/37
Age (days)	275	229	456	133	839	679	1014	988	1290

Fig. 1. Test arrangement (water bath and RCPT cell).

and monitor the temperature during these experiments (see Fig. 1. for test arrangement).

In some cases, the temperature of the bath fluid (water) was raised from 23 ± 2 °C to a specific temperature (up to 90 °C) using a linear temperature rise over the duration of the RCPT (6 h). In other experiments, the temperature of the system was kept constant during the test. For both cases the RCPT was not started until the initial temperature target was achieved and then stabilized as required. As well, a few experiments were done by decreasing the temperature (to 5 °C). For those cases, the temperature of the cell was monitored with independent thermometers. Care was taken to assure that a short circuit would not happen at the electrical connectors of the cells when the cells were immersed.

The limits for the temperatures applied artificially during the test were consistent with those recommended in ASTM C1202 where to avoid damage to the cells and avoid boiling of the solution, the maximum temperature (T_{6h}) is kept below 90 °C. Also, some commercial RCPT machines are programmed to disconnect the cell if the temperature of the solution rises higher than 90 °C or if the electrical current becomes greater than a specified value, for example, 500 mA.

3. Results

3.1. Joule effect

Results from this study as shown in Fig. 2 confirm the proportionality between total charge ($Q_{c_{6h}}$) and the temperature increment, δT, which is the difference between the final temperature, T_{6h}, and the initial temperature, T_o, in the test. The linear correlation is very good (R^2=.995) in the range of coulombs obtained in this study. This correlation is maintained at all times during the test as shown in

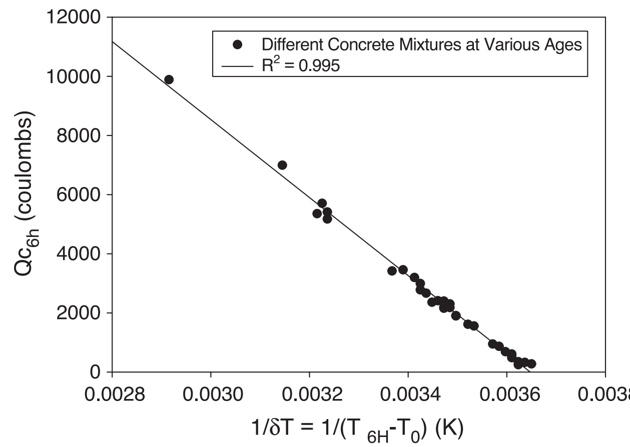

Fig. 2. Correlation between total charge and temperature at 6 h.

Fig. 3. It should be clarified that T_o is the room temperature (23 ± 2 °C); otherwise, δT is the difference between T_{6h} and the room temperature. In addition, when the system is set to a target temperature (e.g., 52 °C) before the test starts and it is kept constant during the test, then δT is equal to the target temperature. As will be seen later, the linear correlation does not mean that if a correction for heat were done, all types of concrete would come to the same total charge value.

3.2. Temperature effect (water bath experiments)

Fig. 4 presents the results for the concrete tested following both water bath procedures. The trend is similar for all these concretes, where the increment of the total charge after 6 h is the invariable result of an increment in temperature. The diagonal line drawn on this graph corresponds to the linear correlation between total charge and the increment in temperature during the RCPT without artificially induced heating.

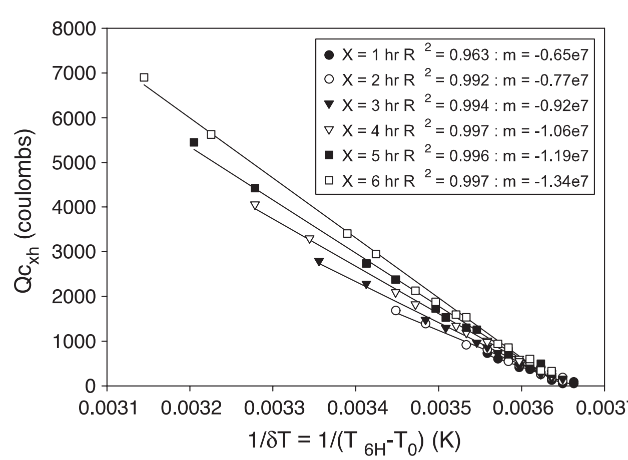

Fig. 3. Correlation between total charge and temperature at different times during the RCPT.

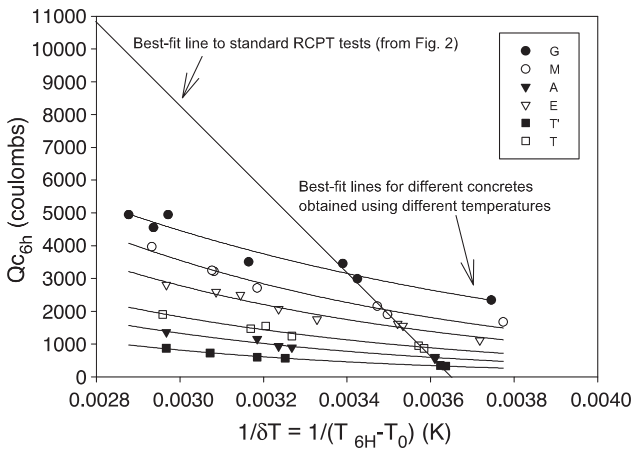

Fig. 4. Effect of temperature on the total charge of various concretes.

3.3. Joule effect equation for RCPT

Based on Fig. 4, the corresponding curves for each concrete were analyzed and fitted using commercial curve-fitting software. One general equation (Eq. (2)) was proposed which gives a corrected total charge value of concrete specimens as if the temperature during the test were kept constant at 23 ± 2 °C. The equation was found to hold well over the range of temperature tested.

$$Q_o = e^{[\ln(Q_{c_{6h}}) + \beta(1/\delta T - 1/273)]} \quad (2)$$

where Q_o is the total corrected charge without the Joule effect (coulombs), $Q_{c,6h}$ is the measured total charge at 6 h adjusted to the standard cross-sectional sample area (coulombs), β is an experimental constant found to be equal to 1245 for these concretes and δT is the temperature increment during the 6-h test ($T_{6h} - T_o$) (degrees Kelvin).

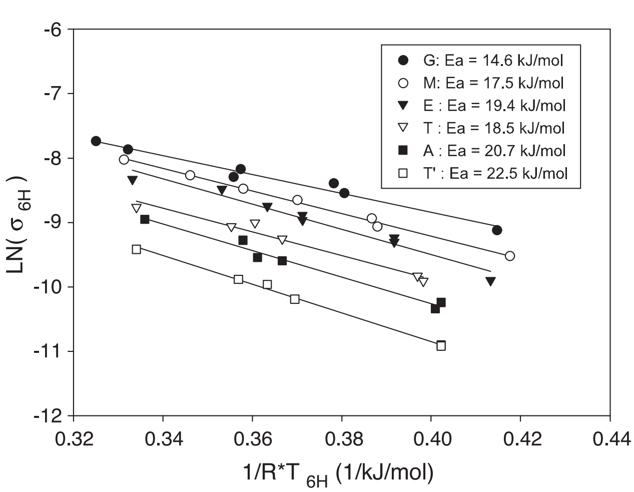

Fig. 5. Arrhenius plot for two types of temperature regimes.

Table 2
Temperature coefficient on resistivity

	Mix code					
	G	M	A	E	T	T′
α (1/°C)	0.0175	0.0179	0.0225	0.0205	0.0209	0.0229
R^2	0.979	0.989	0.856	0.984	0.946	0.945

3.4. Activation energy and temperature coefficient using RCPT

Even though other authors have studied the activation energy of cement-based materials using the AC impedance technique [35,36], no references were found where attempts have been made to evaluate the activation energy of concretes using the RCPT. Since the conductivity of concrete depends on the mobility of ions present in the pore fluid, it is possible to calculate the activation energy using the Arrhenius equation. In this case, the activation energy (E_a) is the activation energy of the migration process related to the movement of ions due to the passage of current. Fig. 5 represents a typical Arrhenius graph for evaluating activation energy (E_a). In this case, the natural logarithm of conductivity (calculated from the current obtained at 6 h) was plotted against inverse temperature and the value of activation energy was calculated from the slope of the line. Activation energy values between 15 and 22 kJ/mol were obtained.

On the other hand, concrete is said to have a negative temperature coefficient of resistance (decrease of resistance with an increase in temperature) [24]. Table 2 shows the temperature coefficients for those concretes that were tested in the water bath and found to have a linear change in resistivity with change in temperature. These values were obtained by plotting the evolution of resistivity values (calculated from the current evolution with time) versus temperature during the test.

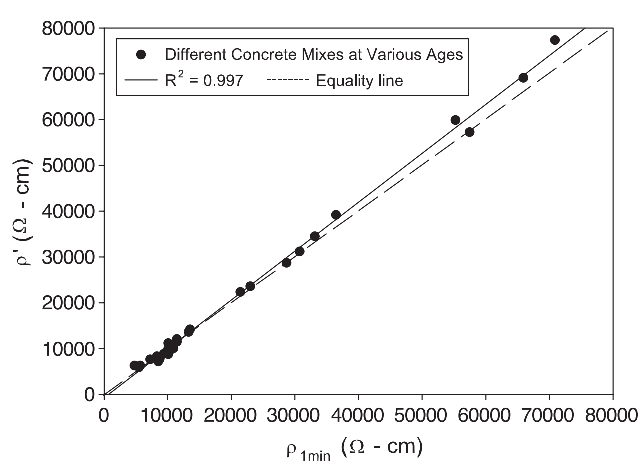

Fig. 6. Correlation between the Heinrichson–Rash formula for resistivity (ρ') and the 1-min resistivity (ρ_{1min}).

Table 3
Summary of main results

Specimen code	Area (cm^2)	Thickness (cm)	Voltage (V)	Current (A)		Resistivity (Ω cm)			Conductivity (μS/cm)		Temperature (°C)			Charge passed (C)		
				I (1 min)	I (6 h)	ρ (1 min)	ρ (6 h)	ρ'	σ (1 min)	σ (6 h)	T_o	T_{6h}	δT	$Q_{c,6h}$	$Q_{c.30mi}$ × 12	Q_o
G1	80.2	5.09	60	0.114	0.184	8,293	5,138	8,302	121	195	24.0	43.0	19.0	2,990	2,279	2,222
G2	80.1	5.03	60	0.132	0.217	7,238	4,403	7,662	138	227	23.0	45.0	22.0	3,456	2,596	2,460
G3	80.0	5.05	60	0.120	0.104	7,921	9,139	7,744	126	109	23.0	17.0	− 6.0	2,344	2,413	2,597
G4	80.0	5.03	60	0.134	0.365	7,121	2,614	11,724	140	382	21.5	89.0	67.5	4,553	2,712	1,844
G5	80.2	4.99	60	0.116	0.241	8,313	4,001	11,119	120	250	22.0	65.0	43.0	3,503	2,367	1,883
G6	80.1	5.03	60	0.138	0.417	6,924	2,291	11,519	144	436	22.5	97.0	74.5	4,947	2,813	1,861
G7	80.0	5.05	60	0.209	0.271	4,548	3,507	3,507	220	285	63.5	63.5	63.5[a]	4,952	4,262	2,094
M1	80.5	5.00	60	0.096	0.127	10,063	7,606	11,192	99	131	23.0	38.0	15.0	2,155	1,840	1,699
M2	80.5	5.02	60	0.084	0.111	11,454	8,668	12,113	87	115	24.0	37.0	13.0	1,904	1,625	1,548
M3	80.5	5.02	60	0.103	0.247	9,341	3,895	12,761	107	257	23.0	74.5	51.5	3,215	1,996	1,559
M4	80.4	5.05	60	0.106	0.070	9,012	13,646	10,925	111	73	23.0	15.0	− 8.0	1,674	2,031	1,921
M5	80.1	5.01	60	0.093	0.200	10,315	4,796	12,784	97	208	22.0	63.0	41.0	2,708	1,827	1,493
M6	80.2	5.04	60	0.106	0.313	9,007	3,050	13,739	111	328	22.0	90.0	68.0	3,969	2,142	1,599
M7	80.4	5.05	60	0.164	0.168	5,825	5,686	5,686	172	176	52.0	52.0	52[a]	3,248	3,120	1,566
A1	80.3	5.01	60	0.029	0.031	33,161	31,022	34,517	30	32	23.0	27.0	4.0	556	539	521
A2	79.9	5.03	60	0.031	0.034	30,745	28,032	31,212	33	36	22.0	26.0	4.0	607	580	568
A3	80.3	5.01	60	0.033	0.069	29,142	13,937	33,025	34	72	24.0	60.0	36.0	933	639	548
A4	80.2	5.04	60	0.032	0.065	29,836	14,689	32,962	34	68	22.0	55.0	33.0	897	626	549
A5	80.1	5.03	60	0.033	0.124	28,954	7,705	32,558	35	130	21.0	85.0	64.0	1,362	679	573
A6	80.3	5.07	60	0.035	0.089	27,151	10,677	28,459	37	94	22.0	63.0	41.0	1,152	710	635
E1	82.0	5.01	60	0.074	0.096	13,271	10,230	13,629	75	98	23.0	34.0	11.0	1,618	1,427	1,356
E2	82.0	4.99	60	0.073	0.090	13,506	10,955	14,207	74	91	24.0	34.0	10.0	1,558	1,403	1,326
E3	81.7	4.88	60	0.076	0.243	13,217	4,134	17,012	76	242	24.0	88.0	64.0	2,807	1,489	1,181
E4	82.2	4.89	60	0.075	0.209	13,448	4,826	13,928	74	207	22.5	67.5	45.0	2,499	1,470	1,311
E5	80.9	4.95	60	0.068	0.156	14,421	6,286	15,061	69	159	22.0	58.0	36.0	2,067	1,356	1,215
E6	81.7	4.83	60	0.067	0.051	15,148	19,900	17,820	66	50	22.0	18.0	− 4.0	1,116	1,291	1,194
E7	80.8	4.92	60	0.065	0.126	15,159	7,820	15,412	66	128	23.5	51.0	27.5	1,748	1,285	1,152
E8	81.4	4.89	60	0.127	0.133	7,864	7,510	7,510	127	133	51.0	51.0	51[a]	2,591	2,571	1,264
T'1	79.6	4.80	60	0.016	0.081	62,188	12,284	50,994	16	81	23.0	87.0	64.0	873	353	367
T'2	81.4	4.80	60	0.017	0.052	59,853	19,567	51,830	17	51	23.0	64.0	41.0	601	324	331
T'3	80.6	4.85	60	0.015	0.047	66,474	21,215	48,806	15	47	23.5	58.0	34.5	568	316	341
T'4	82.0	4.82	60	0.033	0.036	30,932	28,354	28,354	32	35	52.5	52.5	52.5	729	653	349
T'5	79.5	4.88	60	0.017	0.018	57,498	54,303	57,281	17	18	24.0	26.0	2.0	331	330	320
T'6	79.8	4.82	60	0.018	0.018	55,187	55,187	59,803	18	18	23.0	26.0	3.0	346	346	329
T1	80.4	4.99	60	0.049	0.119	19,729	8,124	20,820	51	123	21.5	60.5	39.0	1,552	973	878
T2	80.8	4.95	60	0.046	0.153	21,291	6,401	27,305	47	156	22.0	87.0	65.0	1,908	926	794
T3	81.6	4.94	60	0.042	0.095	23,597	10,433	23,411	42	96	22.0	55.0	33.0	1,245	834	761
T4	80.2	4.95	60	0.044	0.113	22,094	8,603	23,509	45	116	23.0	65.5	42.5	1,472	891	796
T5	81.9	4.99	60	0.046	0.053	21,408	18,581	22,356	47	54	23.0	30.0	7.0	951	886	849
T6	79.7	4.95	60	0.042	0.048	23,001	20,126	23,597	43	50	23.0	29.0	6.0	865	808	784
W	80.1	5.00	60	0.212	0.461	4,534	2,085	6,299	221	480	24.0	69.0	45.0	6,988	4,392	3,665
C7	80.2	5.04	60	0.015	0.014	65,896	67,288	69,102	15	15	25.0	26.0	− 1.0	277	280	272
C13	80.3	5.07	60	0.013	0.013	70,870	71,402	77,334	14	14	24.0	27.0	− 2.0	247	252	235

[a] Target temperature as defined in Section 3.1.

3.5. Resistivity from RCPT method

Values of resistivity, ρ', calculated from the Heinrichson–Rash (H-R) formula, Eq. (3) (which allows conversion of the resistivity of a refractory material from one temperature to another [24]), were compared with the values of resistivity obtained from current values measured at 1 min, obtaining good correlation (R^2=.997) (Fig. 6).

$$\rho' = \rho_{6h} e^{a(1/T_o - 1/T_{6h})} \quad (3)$$

where ρ' and ρ_{6h} are resistivities (Ω cm) at temperatures T_o and T_{6h}, respectively, and a is a constant equal to 2180 [24] (2370 from this study).

A summary of the results obtained in this study is presented in Table 3.

4. Discussion

It is well known that the RCPT has some drawbacks including the heat effect that makes the total coulomb values unrealistic when testing high water–cement-ratio

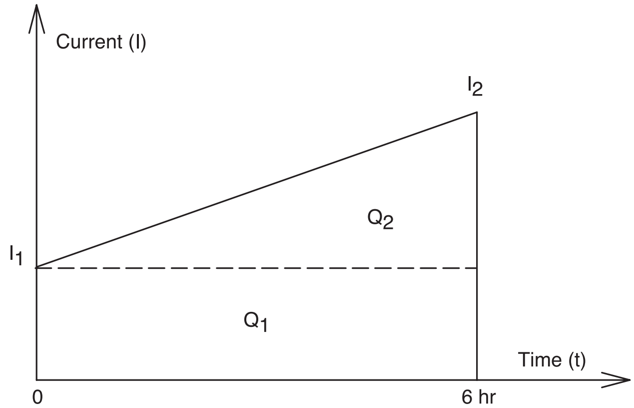

Fig. 7. Current evolution for linear temperature ramp regime.

concrete. The idea of modifying the ASTM C1202 standard is economically more favourable than creating a totally new test due to the widespread use of RCPT equipment in North America. Therefore, changes in the type of measured data (conductivity instead of total charge) and time (a few minutes rather than 6 h) are options that provide an improvement to the existing test. The correlation between total charge and conductivity should be confirmed if it is expected to use the same equipment for the modified RCPT standard. In the past, some correlations between total charge and conductivity (resistivity) have been found to be erratic [6], while others were successful at low and moderate coulomb values [7]. The Joule effect has been the major obstacle in confirming the expected theoretical relationship between total charge and conductivity using Ohm's law. Thus, the Arrhenius analysis allows comparison of those two parameters without the heat effect. Based on the results of this study, the correlation between total charge, corrected for the heat effect, and conductivity at 1 min holds well (R=.988). For the total charge to be corrected, concrete specimens from the same mix have to be tested at different temperatures, so that the heat is the main variable during the test.

4.1. Joule effect

In the RCPT method, the potential (60 V) and testing time are constant (6 h), therefore the quantity of heat released will be directly proportional to the electric current. Moreover, assuming that Taylor–Richmann law (which quantifies the heat required to raise the temperature of the specimen with mass M from T_1 to T_2) (Eq. (4)) can be coupled with the Joule equation (Eq. (1)), then the linear correlation between electric current and temperature becomes clear and can be developed as follows [26–33]:

$$J = \Gamma M(\delta T) \tag{4}$$

where J is the heat (joules), Γ is a coefficient of proportionality, M is the mass of concrete (kg) and δT is the temperature increment during the test ($T_{6h} - T_o$) (degrees Kelvin).

From Eq. (1): $J = EIt$, then, $EIt \approx \Gamma M(\delta T)$.

Also, E, t and M can be considered constants in the RCPT, and the coefficient Γ will depend on the ions present in the pore fluid and it might vary over a small range for different concretes. Then,

$$I \approx \xi(\delta T) \tag{5}$$

where ξ is a constant equal to $\Gamma M/Et$.

4.2. Temperature effect (water bath experiments)

Two regimes were used to heat the cells using the programmable water bath. The first one consisted of incrementing the temperature using a linear ramp, from the standard laboratory conditions up to a target temperature, during 6 h. The second regime involved keeping a target temperature constant during the test. In both cases, the points fit one defined curve. Therefore, it can be inferred that the total charge measured when the temperature increases from T_1 to T_2 is similar to the total charge obtained when a temperature T_3 is kept constant during the test (as long as the temperature T_3 corresponds approximately to the average of both temperatures, T_1 and T_2). This can be explained mathematically by calculating the areas underneath the curve (Figs. 7 and 8) and assuming a linear behaviour of the electric current with time.

From Fig. 7: $Q_A = Q_1 + Q_2 = I_1 t + [(I_2 - I_1/2)t] = (t/2)(I_1 + I_2)$.

From Fig. 8: $Q_B = I_3 t$, if $I_3 = (I_1 + I_2)/2$, then $Q_A = Q_B$.

4.3. Joule effect equation for RCPT

Some authors have proposed using the 30-min charge multiplied by 12 as an option to minimize or avoid the effect of heat in the total 6-h test charge [4,23]. Fig. 9 compares the total charge passed including the heat effect versus the total charge calculated from 12 times the 30-min charge, and the total charge from the equation proposed in this paper (Eq. (2)). Some differences in the results using these two

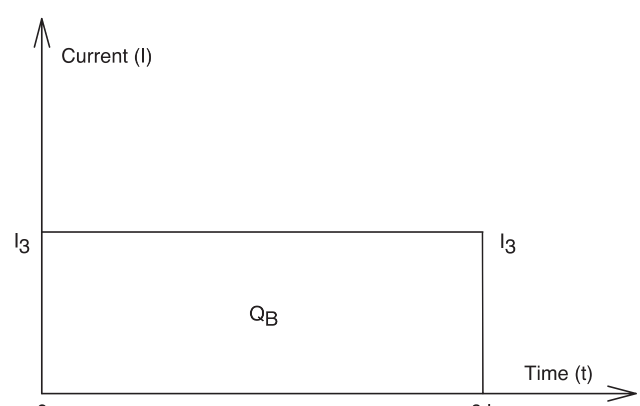

Fig. 8. Current evolution during constant temperature regime.

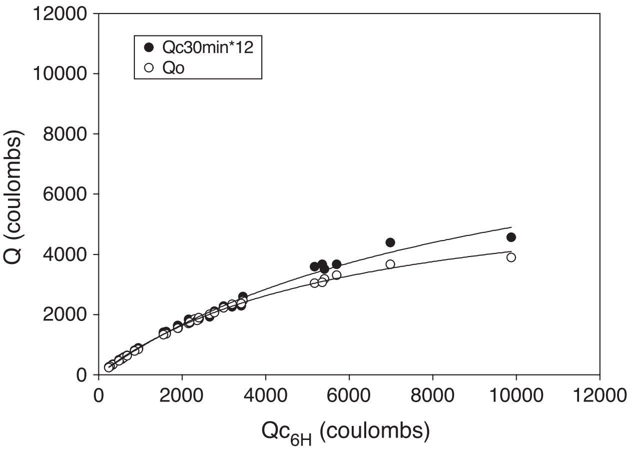

Fig. 9. Comparison between the total charge calculated from the 30-min charge multiplied by 12 and the total charge from Eq. (2) (Q_o).

approaches were observed at high coulomb values. These discrepancies can be related to the fact that even at 30 min, concretes with high coulomb values will generate considerable heat (up to 40 °C).

The change of coulomb values and conductivity with temperature observed in Figs. 4 and 5, respectively, gives some insights into the change in the microstructure of the concrete and pore fluid conductivity during the RCPT. It seems that for low water–cement-ratio mixtures, the effect of temperature on current flow is evident. It might happen that the discontinuity of the pore system is affected allowing higher flow of current through the concrete, and also that the ions in the pore fluid conduct more current due to their higher mobility at high temperatures. For high water–cement-ratio mixtures, the concentration of ions in the pore fluid might not be enough to conduct more current and perhaps possible damage of the microstructure occurs during the test; therefore, the conductivity will not increase in the same proportion as expected.

4.4. Activation energy and temperature coefficient using RCPT

The activation energies calculated from Fig. 5 are conceptually consistent with the flow of current (shown in Fig. 4); that is, the larger the activation energy, the higher the temperature needed to increase the current flow appreciably. Values for the temperature effect on resistivity of concrete were found to be in the order of 0.019/°C (average). Based on this study, the use of linear equations (i.e., $\rho_2 = \rho_1/[1 + \alpha(\Delta T)]$ or $R_1 = R_2[1 + \alpha(\Delta T)]$ [25]) to calculate the temperature coefficient of concretes should be restricted to temperatures no higher than 35 °C. Beyond this temperature the changes are nonlinear with temperature, so these equations are no longer applicable (see Fig. 10).

4.5. Conductivity from RCPT method

Both resistivity and conductivity are inherent properties of most materials and their values can be useful for assessing the quality of concretes related to durability. The issue is to decide at which moment during the RCPT these properties should be evaluated. Fig. 11 shows the correlation between the 1-min conductivity and the total charge without any heat effect, and its good correlation appears to allow comparison of different concretes by only running the RCPT for a few minutes. A proposed ASTM standard, which is a modification of the ASTM C1202, would measure the 1-min conductivity. However, because the measured conductivity is related to both the connectivity of the pore system and the conductivity of the pore fluid, the "formation factor" concept could be used in the analysis of the results to assess the effect of the microstructure of the concrete on its conductivity as suggested by other authors [35].

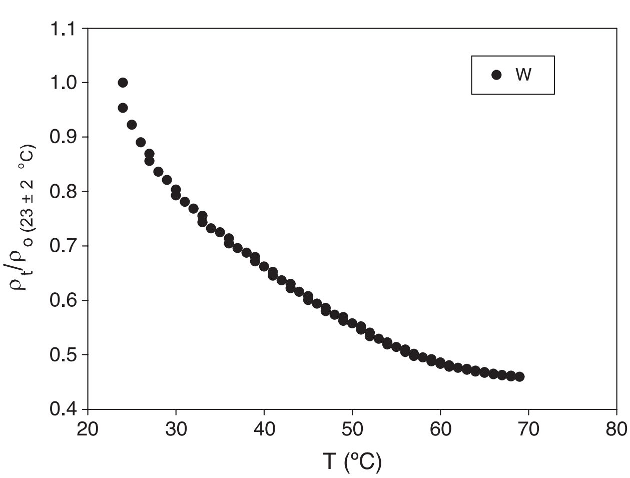

Fig. 10. Changes in resistivity with temperature during the RCPT.

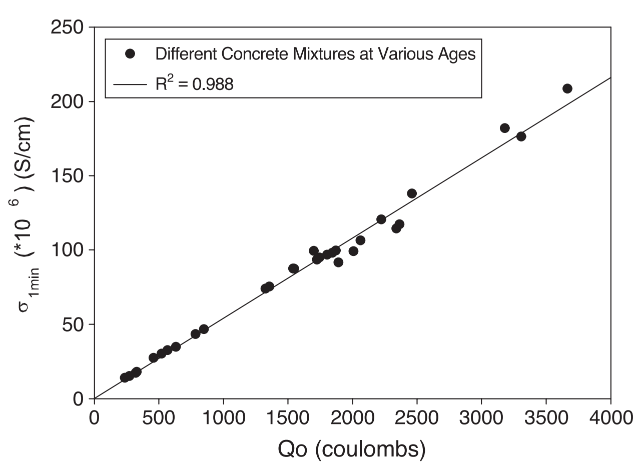

Fig. 11. Correlation between the conductivity at 1 min and the total charge from Eq. (2) (Q_o).

5. Conclusions

The flow of current through concrete is consistent with the electrical proportionalities (i.e., Ohm's law), so any correlation between temperature and current or among other variables is expected to hold. Thus, the linear correlation between total charge and temperature was evident using the RCPT. Also, an equation was suggested to account for the Joule effect and it was shown to work well for temperatures up to 90 °C.

Activation energies obtained from the RCPT seem to differ from those obtained from bulk diffusion tests. Linear equations to calculate the temperature coefficient of resistivity are not recommended for concretes that during the RCPT reach temperatures higher than 35 °C. The Heinrichson–Rash formula applied fairly well for concretes.

The results presented have shown the validity of adopting the 1-min conductivity test, using the RCPT test equipment, as a practical way of improving the current ASTM C1202 standard. (Note: A ballot to adopt this modification is under way at the time of writing)

The 1-min conductivity was found to be very helpful in understanding the ideal behaviour of concrete tested using the RCPT when the effect of temperature in the pore fluid and microstructure are not considered. Finally, it is recommended to perform more work related to the correlation between conductivity and permeability of concrete.

Acknowledgements

The authors want to thank Michelle Nokken, Kyle Stanish and Medhat Shehata for their helpful suggestions and discussions, and also those in the Concrete Materials Group who indirectly or directly were involved by testing or supplying the concrete used in this project.

References

[1] D. Whiting, Rapid measurement of the chloride permeability of concrete, Public Roads 45 (3) (1981) 101–112.
[2] D. Whiting, T.M. Mitchell, History of the rapid chloride permeability test, Transp. Res. Rec. 1335 (1992) 55–62.
[3] ASTM C1202-97, Electrical indication of concrete's ability to resist chloride ion penetration, ASTM Vol.04.02, ASTM, Philadelphia, PA, 2002, pp. 654–659.
[4] P.F. McGrath, R.D. Hooton, Re-evaluation of the AASHTO T259 90 day salt ponding test, Cem. Concr. Res. 29 (1999) 1239–1248.
[5] P.F. McGrath, R.D. Hooton, Influence of binder composition on chloride penetration resistance of concrete, ACI SP170, (1997) 331–348.
[6] K.A. Snyder, C. Ferraris, N.S. Martys, E.J. Garboczi, Using the impedance spectroscopy to assess the viability of the rapid chloride test for determining concrete conductivity, J. Res. Natl. Inst. Stand. Technol. 105 (4) (2000) 497–509.
[7] R. Feldman, L.R. Prudencio Jr., G. Chan, Rapid chloride permeability test on blended cement and other concretes: correlation between charge, initial current and conductivity, Const. Build. Mater. 13 (1999) 149–154.
[8] C.C. Yang, S.W.C. Huang, The relationship between charge passed and the chloride-ion concentration in concrete using steady-state chloride migration test, Cem. Concr. Res. 32 (2002) 217–222.
[9] T.H. Wee, A.K. Suryavanshi, S.S. Tin, Evaluation of rapid chloride permeability test (RCPT) results for concrete containing mineral admixtures, ACI Mater. J. 97 (2) (2000) 221–232.
[10] T.H. Wee, A.K. Suryavanshi, S.S. Tin, Influence of aggregate fraction in the mix on the reliability of the rapid chloride permeability test, Cem. Concr. Compos. 21 (1999) 59–72.
[11] Z. Liu, J.J. Beaudoin, An assessment of the relative permeability of cement systems using AC impedance techniques, Cem. Concr. Res. 29 (1999) 1085–1090.
[12] P.E. Streicher, M.G. Alexander, A chloride conduction test for concrete, Cem. Concr. Res. 25 (6) (1995) 1284–1294.
[13] T. Zhang, O.E. Gjørv, An electrochemical method for accelerated testing of chloride diffusivity in concrete, Cem. Concr. Res. 24 (8) (1994) 1534–1548.
[14] R.F. Feldman, G.W. Chan, R.J. Brousseau, P.J. Tumidajski, Investigation of the rapid chloride permeability test, ACI Mater. J. 91 (2) (1994) 246–255.
[15] R.J. Detwiler, C.A. Fapohunda, J. Natale, Use of supplementary cementing materials to increase the resistance to chloride ion penetration of concretes cured at elevated temperatures, ACI Mater. J. 91 (1) (1994) 63–66.
[16] C. Andrade, Calculation of chloride diffusion coefficients in concrete from ionic migration measurements, Cem. Concr. Res. 23 (3) (1993) 724–742.
[17] R.J. Detwiler, K.O. Kjellsen, O.E. Gjørv, Resistance to chloride intrusion of concrete cured at different temperatures, ACI Mater. J. 88 (1) (1991) 19–24.
[18] R.J. Detwiler, C.A. Fapohunda, A comparison of two methods for measuring the chloride ion permeability of concrete, Cem., Concr. Aggreg. 15 (1) (1993) 70–73.
[19] J.G. Cabrera, P.A. Claisse, Measurement of chloride penetration into silica fume concrete, Cem. Concr. Compos. 12 (1990) 157–161.
[20] C. Andrade, M.A. Sanjuán, Experimental procedure for the calculation of chloride diffusion coefficients in concrete from migration tests, Adv. Cem. Res. 6 (23) (1994) 127–134.
[21] M.-H. Zhang, O.E. Gjørv, Permeability of high-strength lightweight concrete, ACI Mater. J. 88 (5) (1991) 463–469.
[22] P. McGrath, Development of test methods for predicting chloride penetration into high performance concrete, PhD Thesis, University of Toronto, 1996.
[23] K.D. Stanish, R.D. Hooton, M.D.A. Thomas, Testing the chloride penetration resistance of concrete: a literature review, FHWA Contract DTFH61-97-R-00022, 1997, pp. 1–30.
[24] H.W. Whittington, J. McCarter, M.C. Forde, The conduction of electricity through concrete, Mag. Concr. Res. 114 (33) (1981) 48–60.
[25] G. Wilcox, C.A. Hesselberth, Electricity for Engineering Technology, Allyn and Bacon, Boston, 1970.
[26] W.R. Smythe, Static and Dynamic Electricity, third ed., McGraw-Hill, New York, 1968.
[27] S. Glasstone, Textbook of Physical Chemistry, second ed., D. Van Nostrand, Toronto, 1950.
[28] M.A. Paul, Principles of Chemical Thermodynamics, McGraw-Hill, New York, 1951.
[29] S. Glasstone, An Introduction to Electrochemistry, D. Van Nostrand, New York, 1947.
[30] H.J. Creighton, Principles and Applications of Electrochemistry, Vol. 1, Wiley, London, 1943.
[31] W.J. Moore, Physical Chemistry, fourth ed., Prentice-Hall, Englewood Cliffs, NJ, 1972.
[32] H.S. Harned, B.B. Owen, The Physical Chemistry of Electrolytic Solutions, third ed., Reinhold, New York, 1958.

[33] D.A. MacInnes, The Principles of Electrochemistry, Reinhold, New York, 1939.
[34] P.F. McGrath, R.D. Hooton, Influence of voltage on chloride diffusion coefficients from chloride migration tests, Cem. Concr. Res. 26 (8) (1996) 1239–1244.
[35] W.J. McCarter, G. Starrs, T.M. Chrisp, Electrical conductivity, diffusion, and permeability of Portland cement-based mortar, Cem. Concr. Res. 30 (2000) 1395–1400.
[36] T.M. Chrisp, G. Starrs, W.J. McCarter, E. Rouchotas, J. Blewett, Temperature–conductivity relationships for concrete: an activation energy approach, J. Mater. Sci. Lett. 20 (2001) 1085–1087.